https://doi.org/10.5194/egusphere-2023-1068
Preprint. Discussion started: 16 June 2023
© Author(s) 2023. CC BY 4.0 License.

Exploring the relationship between sea-ice and primary production in the Weddell Gyre using satellite and Argo-float data

Clara Celestine Douglas[1,2], Nathan Briggs[2], Peter Brown[2], Graeme MacGilchrist[3,4], and Alberto Naveira Garabato[1]

[1]Ocean and Earth Science, University of Southampton, Southampton, UK
[2]Ocean BioGeosciences, National Oceanography Centre, Southampton, UK
[3]Atmospheric and Oceanic Science, Princeton University, Princeton, NJ, USA
[4]Earth and Environmental Sciences, University of St Andrews, St Andrews, UK

Correspondence: Clara Douglas (C.C.Douglas@soton.ac.uk)

Abstract. Some of the highest rates of primary production across the Southern Ocean occur in the seasonal ice zone (SIZ), making this area of prominent importance for both local ecosystems and the global carbon cycle. There, the annual advance and retreat of ice impact light and nutrient availability, as well as the circulation and stratification, imposing a dominant control on phytoplankton growth. In this study, the drivers and variability of net primary production (NPP) in the Weddell Gyre SIZ were assessed using satellite and autonomous biogeochemical float data. Although the highest daily rates of NPP are consistently observed in the continental shelf region (water depths shallower than 2000m), the open ocean region's larger size and longer ice-free season mean that it dominates biological carbon uptake within the Gyre, accounting for 95% of the Gyre's total annual NPP. Variability in the summer maximum ice-free area is the strongest predictor of inter-annual variability in total NPP across the Weddell Gyre (R^2=62%), with greater ice-free area resulting in greater annual NPP. In the shelf region, the return of sea-ice cover controls the end of the productive season. In the open ocean, however, a decline in NPP occurs before the end of the ice-free season ($\sim$ 80 to 120 days after sea-ice retreat), suggesting that, later in the summer season, additional factors such as nutrient availability limit NPP. These results indicate that in a warmer and more ice-free Weddell Gyre, notwithstanding compensating changes in nutrient supply, NPP is likely to be enhanced only up to a certain limit of ice-free days.

1 Introduction

The seasonal ice zone (SIZ) in the Southern Ocean (SO) plays an important but poorly quantified role in the net uptake and sequestration of carbon into the oceans on a range of timescales (Sigman et al., 2010; Brown et al., 2015; Van Heuven et al., 2014; Bushinsky et al., 2019). In this region, some of the highest rates of primary production across the SO are observed (Arrigo et al., 2008b). Consequently, biological activity is considered to be key in determining the region's net carbon sink via the biological carbon pump (Brown et al., 2015; MacGilchrist et al., 2019; Henley et al., 2020). The biological carbon pump begins with the fixation of carbon through photosynthesis by phytoplankton, which lowers the levels of carbon dioxide in the surface ocean, driving uptake of carbon into the ocean from the atmosphere (Hauck et al., 2015). The fate of this fixed carbon (recycled in the surface ocean by heterotrophs or exported to depth) determines the strength and sign of the SO carbon sink

https://doi.org/10.5194/egusphere-2023-1068
Preprint. Discussion started: 16 June 2023
© Author(s) 2023. CC BY 4.0 License.

(Arteaga et al., 2019; Ducklow et al., 2018; Sigman et al., 2010; Boyd et al., 2019). Furthermore, primary production forms the base of a rich and efficient food web in the SIZ, with high productivity regions supporting areas of ecological significance (Hindell et al., 2020), and commercially important species including krill, toothfish and squid (Trebilco et al., 2020).

Sea-ice dynamics play a critical role in primary production in the SIZ by attenuating light and altering stratification, mixing, and nutrient delivery (McGillicuddy et al., 2015; Gupta et al., 2020; Twelves et al., 2021). Much of our understanding of these impacts is derived from regional, small-scale, and modeling studies (e.g. Bisson and Cael, 2021; Hague and Vichi, 2021; Schultz et al., 2021; Taylor et al., 2013; von Berg et al., 2020; Giddy et al., 2021). However, observational evidence for their basin-scale spatiotemporal relationship is lacking. In light of observed and anticipated changes in the climate of the SIZ (Kumar et al., 2021; Ludescher et al., 2019; Casagrande et al., 2023), the need for a deeper understanding of this relationship – and the broader controls on net primary production (NPP) in this region – is pressing. Climate models from Coupled Model Intercomparison Project Phase 5 and 6 (CMIP5 and CMIP6) project a decline in Antarctic sea-ice area and concentration as a response to anthropogenic climate change (Casagrande et al., 2023). However, low confidence in projections, due to the complexity of ocean-ice-atmosphere systems, means that exact estimates of decline are uncertain (Casagrande et al., 2023; Meredith et al., 2019). It is anticipated, therefore, that changes in primary production in the SIZ will follow in the coming decades, with concomitant impacts on carbon uptake and ecosystem health. However, the crucial gaps in our understanding of the drivers of NPP in the SIZ mean that large uncertainty remains about the nature and extent of these changes (Campbell et al., 2019; Henley et al., 2020; Kim and Kim, 2021; Pinkerton et al., 2021; Séférian et al., 2020; Henson et al., 2022).

The Weddell Gyre is one of a few regions of deep and bottom water formation, and it has largely been thought that the transportation of these water masses to depth was the principal pathway for vast quantities of carbon (taken up through the solubility and biological carbon pumps) to be sequestered from the SO (Jullion et al., 2014; Meredith et al., 2014; Van Heuven et al., 2014). However, it has more recently been hypothesised that this may not be the case. Instead, the Weddell Gyre's net CO_2 sink may be driven by biological carbon uptake in the offshore central Gyre, where the accumulation of respired carbon at mid-depths within local Circumpolar Deep Water, and circulation of this enriched water mass out of the Gyre, provide a significant pathway for carbon sequestration north of the Gyre (MacGilchrist et al., 2019). Many SO biological carbon pump studies have focused on coastal and shelf regions, such as highly productive polynyas (e.g. McGillicuddy et al., 2015; Arrigo et al., 2015). However, the offshore (open ocean) area of the Weddell Gyre exhibits high annual NPP in comparison to shelf regions and has been documented as one of the most productive marginal ice zones in the Southern Ocean (Arrigo et al., 2008b). As such, the interaction between biology and circulation in the off-shore area of this SO region is particularly important, and it is vital to advance understanding of what drives these processes now to improve prediction of how they may change in the future.

Given the importance of biological carbon uptake in the Weddell Gyre for local ecosystems and the global carbon cycle, this paper characterises and quantifies the basin-scale relationship between NPP and sea-ice using both satellite products and *in situ* observations from Biogeochemical (BGC) Argo floats. In Sect. 2 we describe our data and methods and highlight, and quantify uncertainties associated with our approach. In Sect. 3 we present a multi-year perspective of NPP in the Weddell Gyre, as well

https://doi.org/10.5194/egusphere-2023-1068
Preprint. Discussion started: 16 June 2023
© Author(s) 2023. CC BY 4.0 License.

as its variability, before discussing the importance of sea-ice and nutrient availability in driving inter-annual variability in NPP in Sect. 4.

2 Data and Methods

2.1 Study Area

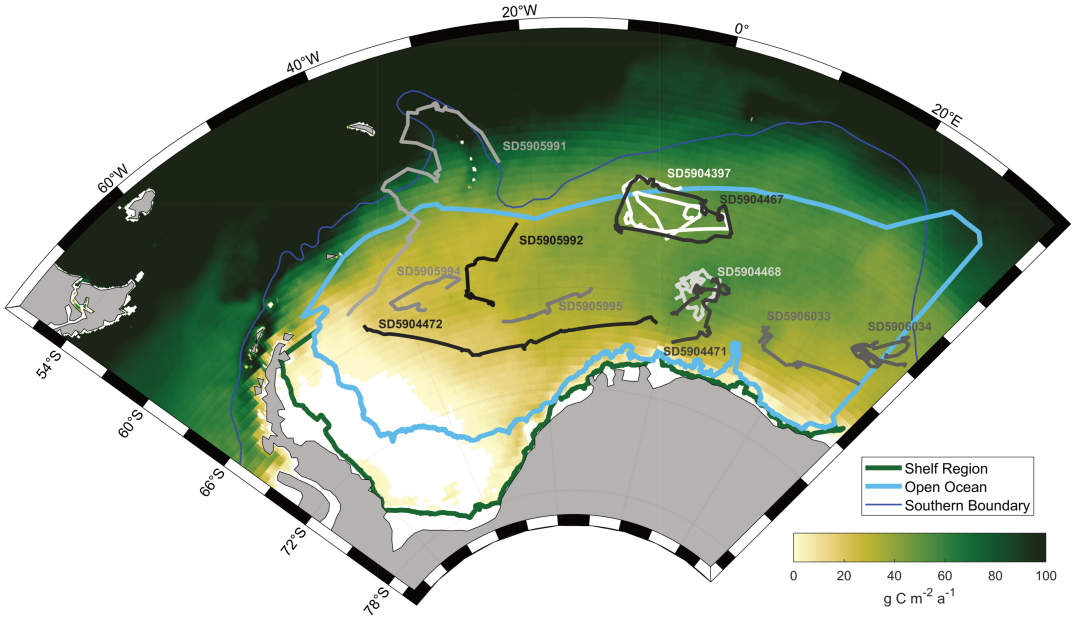

Figure 1. Location of the Weddell Sea, Southern Boundary (dark blue line) and study subregions (blue: open ocean; green: shelf). The 18-year mean area-normalised annual NPP (g C m^{-2}) climatology derived from MODIS-Aqua satellite measurements using the Carbon, Absorption and Fluorescence Euphotic-resolving (CAFE) model is represented by the yellow to green colourmap. White areas represent no data (permanent sea-ice present). SOCCOM float trajectories from 12 BGC-Argo floats are shown in greyscale and labeled with WMO ID.

The Weddell Gyre is a cyclonic gyre located in the Atlantic sector of the SO (Fig. 1; Vernet et al., 2019). Water primarily enters the gyre from the east (Circumpolar Deep Water supplied from the Antarctic Circumpolar Current and leaves toward the north, with its circulation and extent determined by wind forcing and topography (Hoppema, 2004; MacGilchrist et al., 2019; Vernet et al., 2019). Sea-ice extends across almost the entire Weddell Gyre in the winter and retreats in the summer, encompassing the Gyre within the SIZ (Arrigo et al., 2008b; Vernet et al., 2019).

The extent of the study area was defined to align with previous studies of the Weddell Gyre (Jullion et al., 2014; Brown et al., 2015; MacGilchrist et al., 2019). The region is bounded by the Antarctic continent to the south and west and two hydrographic transects to the north and east: the Antarctic Deep Water Rate of Export (ANDREX) cruises, and the CLIVAR quasi-meridional I6S section at 30 °E (Fig. 1; Bacon and Jullion, 2009; Meredith, 2010; Speer and Dittmar, 2008). For the

https://doi.org/10.5194/egusphere-2023-1068
Preprint. Discussion started: 16 June 2023
© Author(s) 2023. CC BY 4.0 License.

purposes of this study, the Weddell Gyre was divided into two subregions: a shelf region (defined as the area with bathymetric depth less than 2000m) and an open-ocean region (depths greater than 2000m). The position of the 2000m isobath was extracted from TerrainBase, a 5-minute resolution global elevation database (National Geophysical Data Center/NESDIS/NOAA/U.S. Department of Commerce., 1995).

2.2 Satellite Data

2.2.1 Sea-Ice

Daily satellite sea-ice concentrations over 2002-2020 were taken from the NOAA/National Snow and Ice Data center (NSIDC) Climate Data Record (Version 4, Meier et al., 2021). The data were obtained on the NSIDC polar stereographic 25 x 25 km grid. Eight-day means of sea-ice concentration (SIC) were calculated to match the NPP and Chlorophyll-a (Chl-a) data temporal resolution. Pixels were defined as ice-free if the SIC was less than 15% (Windnagel et al., 2021). Annual statistics were calculated over austral years 2003-2020, starting July 2002 and ending June 2020. The sea-ice area (SIA) was calculated by multiplying the SIC within each pixel by its area. Ice-free area (IFA) was calculated as the difference between the total area of the Weddell Gyre (and sub-regions) and the SIA.

2.2.2 NPP (and Chlorophyll-a)

Satellite-derived NPP products calculated from MODIS (Moderate-Resolution Imaging Spectroradiometer)-Aqua chlorophyll-a (Chl-a) data were obtained from the Ocean Productivity website (www.science.oregonstate.edu/ocean.productivity/ ; Oregon State University, 2019). We use the NPP product derived using the Carbon, Absorption and Fluorescence Euphotic-resolving (CAFE) model (Silsbe et al., 2016; Westberry and Behrenfeld, 2013). Input data to the CAFE model are cloud-filled via spatial and temporal interpolation prior to calculating NPP. The data resolution is 8-day averages on a 1/12° latitude-longitude grid (2-4km zonal resolution, 8-10km meridional resolution in this region) for the period 2002-2020. The CAFE model is an absorption-based model that considers the amount of energy absorbed by phytoplankton, photoacclimation (how much energy is used to fuel growth or is dissipated), and the efficiency with which energy is converted into biomass. CAFE was chosen over other NPP models as it has the best performance of all the models in SO regions, as assessed in Silsbe et al. (2016). Cloud-filled MODIS-Aqua Chl-a concentration data were also obtained at the same resolution as the NPP data.

In our analysis, we derive a number of quantities from the basic NPP variable provided; *i.e.* the area-normalized, time-mean NPP at each lat-lon (x-y) pixel, for each 8-day period, which we label $\mu \equiv \mu(x,y,t)$. The spatially-averaged NPP for each subregion, i, is defined thus:

$$\overline{\mu}^{x,y}(i,t) = \frac{1}{\mathcal{A}(i,t)} \int\limits_{\mathcal{A}(i,t)} \mu(x,y,t)\, dA \tag{1}$$

where $dA \equiv dxdy$ is the area increment, and $\mathcal{A}(i,t)$ corresponds the areal extent of the ice-free area in each subregion i at time t (as ascertained from data availability in the NPP product). Note that this area is not exactly equivalent to the IFA derived from the sea-ice data. The total Weddell Gyre region corresponds to the area $A(t) = \sum_i \mathcal{A}(i,t)$.

https://doi.org/10.5194/egusphere-2023-1068
Preprint. Discussion started: 16 June 2023
© Author(s) 2023. CC BY 4.0 License.

The "total annual NPP" (N) corresponds to the spatially and temporally integrated carbon uptake over each subregion:

$$N(i,\tilde{t}) = \int_{t_s(\tilde{t})}^{t_e(\tilde{t})} \int_{\mathcal{A}(i,t)} \mu(x,y,t)\, dA\, dt \tag{2}$$

where $\tilde{t}$ is a yearly time increment, defined over the austral year starting in July (t_s) and ending in June of the following calendar year (t_e). Although we include the time-dependence of the areal extent here for consistency, it is irrelevant in this calculation because ice-covered pixels (where $\mu = 0$ automatically) contribute nothing in the area integral. Finally, we note that annual means of the spatially-averaged NPP defined above ($\overline{\mu}^{x,y}$) are also derived over the period of the austral year.

Ocean-colour satellite observations are restricted by the presence of sea-ice and when the solar angle/zenith is too low (below 20°, see Sect. 2.4 for more details). The number of days each pixel was visible to the ocean-colour satellite (and therefore had data recorded) was counted. For the most part, satellite-visible days are approximately equivalent to the number of days from sea-ice melt/retreat to low solar angle.

2.3 Autonomous floats

Eleven autonomous BGC-Argo floats deployed by the Southern Ocean Carbon and Climate Observations and Modelling (SOCCOM) project from 2014 onwards observed at least one complete annual cycle (from July to June) within the study region (Fig. 1). The floats were programmed to profile from 1700-2000m to the surface on 10-day intervals. Data for these floats were obtained from the 21 December 2021 SOCCOM snapshot (https://doi.org/10.6075/J00R9PJW) and interpolated over a 5m vertical grid. SOCCOM provide two Chl-a data products which differ in their fluorescence to Chl-a calibration. The corrected Chl-a product (chl_a_corr), which has a Southern Ocean specific correction applied (Johnson et al., 2017), was used here. Missing surface/shallow Chl-a values were extrapolated (nearest neighbor) from the shallowest data available for each profile (Appendix Fig.A3).

Mean and depth-integrated estimates of Chl-a were calculated from float profiles by integrating binned Chl-a concentrations between the surface to 200m and surface to 20m, with the mean estimates for the 0-20m bin intended to line-up with the approximate optical depth of MODIS-Aqua - i.e. what the satellites likely measured (Fig. A2; Gordon and McCluney, 1975). Under-ice profiles were identified based on criteria used in the ice avoidance algorithm, which prevents a float ascending to the surface if the median temperature between 20-50m is less than -1.78 °C (Bisson and Cael, 2021).

The seasonal cycles of float-observed Chl-a were assessed alongside the timings of sea-ice retreat, sea-ice return, and the date when the solar angle drops below 20°, restricting ocean-colour satellite observation, to get a small-scale (localised) depth-resolved perspective on the drivers of seasonal and annual Chl-a variability. The dates that floats emerged from under ice and returned to under-ice conditions were determined and the length of the ice-covered and ice-free seasons were calculated. The average latitude of each float in March was calculated, and based on this location, the date that the solar angle/zenith would be too low for MODIS-Aqua satellite coverage was determined.

https://doi.org/10.5194/egusphere-2023-1068
Preprint. Discussion started: 16 June 2023
© Author(s) 2023. CC BY 4.0 License.

2.4 Uncertainty estimates for satellite chlorophyll-a and NPP

Satellite estimates of annual NPP should be considered conservative due to the limitations of ocean-colour satellites and NPP products. These potential negative biases in satellite-derived annual NPP arise due to three reasons: 1) sea-ice coverage; 2) low solar angle; and 3) data gaps.

Sea-ice restricts ocean-colour satellites from viewing any production taking place under and within sea-ice (Arrigo and van Dijken, 2004; Peck et al., 2010; Pope et al., 2017). Spatial coverage of the ocean-colour satellite is also increasingly restricted from early March, due to the decreasing solar angle limiting optical view (Pope et al., 2017). This means that much of the surface ocean is not observed by the MODIS-Aqua satellite at the end of the summer period despite much of the region still being ice-free. It is therefore likely that some NPP is being missed at the end of the growing season. As a result, NPP is considered zero during winter, where there is no satellite coverage south of 50 °S due to sea-ice coverage and low solar angle.

Without comprehensive *in situ* measurements of NPP, it is not possible to directly quantify what is missed by satellites. Instead, we use float data to determine how much annual-integrated Chl-a is missed, reasoning that this offers a ballpark figure for the fraction of missed NPP. The proportions of annual Chl-a measured by each float observed when the float was (1) under sea-ice and (2) when the solar angle is less than 20°, limiting satellite view at the end of summer (from mid-March) are summarised in Table 1. At the float locations, only a small proportion of annual Chl-a is present under sea-ice (max 1.1%), while up to 20% (median 9.2%) of annual Chl-a is observed by floats during the time when the ocean-colour satellite was unable to view the surface ocean due to low solar angle (Table 1).

There are areas in the mapped NPP data where the cloud fill algorithm did not complete successfully - where data is absent despite the SIC data indicating that no sea-ice is present. There is also a disparity in the spatial coverage of the NPP products and the Chl-a input data used to derive NPP (Table 1). Some of the input data used in the CAFE algorithm to derive NPP have less extensive spatial coverage than the Chl-a input data and/or don't have data along some ice edges due to satellite observation limitations. This means that there are some areas in the NPP product that suggest there is no NPP occurring despite Chl-a being observed by the satellite. On average over a year, there is a $7.51 \pm 3.47 \times 10^4$ km^2 difference in coverage between Chl-a view and NPP product. This is especially relevant for the shelf region, where many of the coastal polynyas that occur are visible in the input Chl-a data, but are not translated into the NPP data. Therefore shelf integrated NPP values are expected to be underestimated.

Ocean-colour satellites are only able to view the surface of the ocean, meaning Chl-a satellite products do not represent the full euphotic zone/water column inventory (Pope et al., 2017). The CAFE algorithm applies a light saturation model for the mixed layer and assumes a co-varying relationship between the phytoplankton absorption coefficient and light saturation below the mixed layer in order to estimate the vertical structure of Chl-a (and NPP; Silsbe et al., 2016). As a result, the subsurface Chl-a/NPP inventory may not be accurately resolved and may also miss subsurface Chl-a maximum layers, which are potentially highly productive and promote enhanced carbon export in the SO (Baldry et al., 2020). Figure A2 highlights the similarities and dissimilarities in float and satellite Chl-a estimates.

https://doi.org/10.5194/egusphere-2023-1068
Preprint. Discussion started: 16 June 2023
© Author(s) 2023. CC BY 4.0 License.

Table 1. Estimation of uncertainty in ocean-colour satellite NPP data based on complementary BGC-Argo float data and assessment of NPP input data

Reason	Estimate of missed data	Notes
Sea-ice	0 - 1.1% (median 0.2%) annual Chl-a	Percentage of annual Chl-a within surface (0-20m) layer
Low solar angle	0.8 - 20% (median 9.2%) annual Chl-a	Percentage of annual Chl-a within surface (0-20m) layer
Missing data	7.51±3.47 x 10^4 km^2 (∼1.3% of WG region)	Other data (temperature, light) used in the NPP calculation have coarser spatial coverage than Chl-a data, particularly over shelves.

3 Results

3.1 Climatological NPP and sea-ice

Total annual phytoplankton NPP integrated over the entire Weddell Gyre averaged (± standard deviation) 172±34 Tg C a^{-1} between 2003 and 2020, while annual area-normalised production was on average 97±8 mg C m^{-2} a^{-1}. While the open ocean experiences lower daily rates of productivity compared to the shelf region (376±33 mg C m^{-2} d^{-1} compared to 582±99 mg C m^{-2} d^{-1}; Appendix Figure A1), area-normalised annual NPP is in fact higher in the open ocean than in the shelf region (97±8.2 mg C m^{-2} a^{-1}, 68±23 mg C m^{-2} a^{-1} respectively; Fig. 2.A), due to a longer mean ice-free season. As a result, when integrated over time and area, the open ocean accounts for a significant majority of the total carbon taken up by phytoplankton in the Weddell Gyre 99%±1% and dominates the inter-annual variability of NPP seen in the region (Fig 2.B). The total annual NPP in the open ocean is 170±33 Tg C compared to 2±2 Tg C in the shelf region.

The summer maximum IFA for the entire Weddell Gyre averaged 4.89±2.39 x 10^6 km^2 between 2003 and 2020 (the equivalent of 1.18x10^6 km^2 summer sea-ice area). The mean IFA per year for the entire Weddell Gyre averaged 2.29±0.25 x 10^6 km^2 between 2003 and 2020. On average in the shelf region, summer (maximum) IFA was 2.39±0.57 x 10^5 km^2, the mean IFA was 1.03±0.12 x 10^5 km^2. In the open ocean region region, the average summer (maximum) IFA was 4.50±0.22 x 10^6 km^2, mean IFA averaged 2.08±0.23 x 10^6 km^2.

A clear seasonal cycle is seen in both NPP and IFA (Fig. 3). When comparing the mean annual cycle of open water area and total NPP, the rise in NPP coincides with the retreat of sea-ice and increase in the area of ice-free water (Fig. 3). In the shelf region, the peak in NPP occurs at maximum open water area, and the decline in NPP coincides with the formation of sea-ice. However, in the open ocean region, NPP peaks before the maximum open water area is seen and then declines despite the continued expansion of open water, creating a mismatch between NPP and sea-ice coverage from February.

https://doi.org/10.5194/egusphere-2023-1068
Preprint. Discussion started: 16 June 2023
© Author(s) 2023. CC BY 4.0 License.

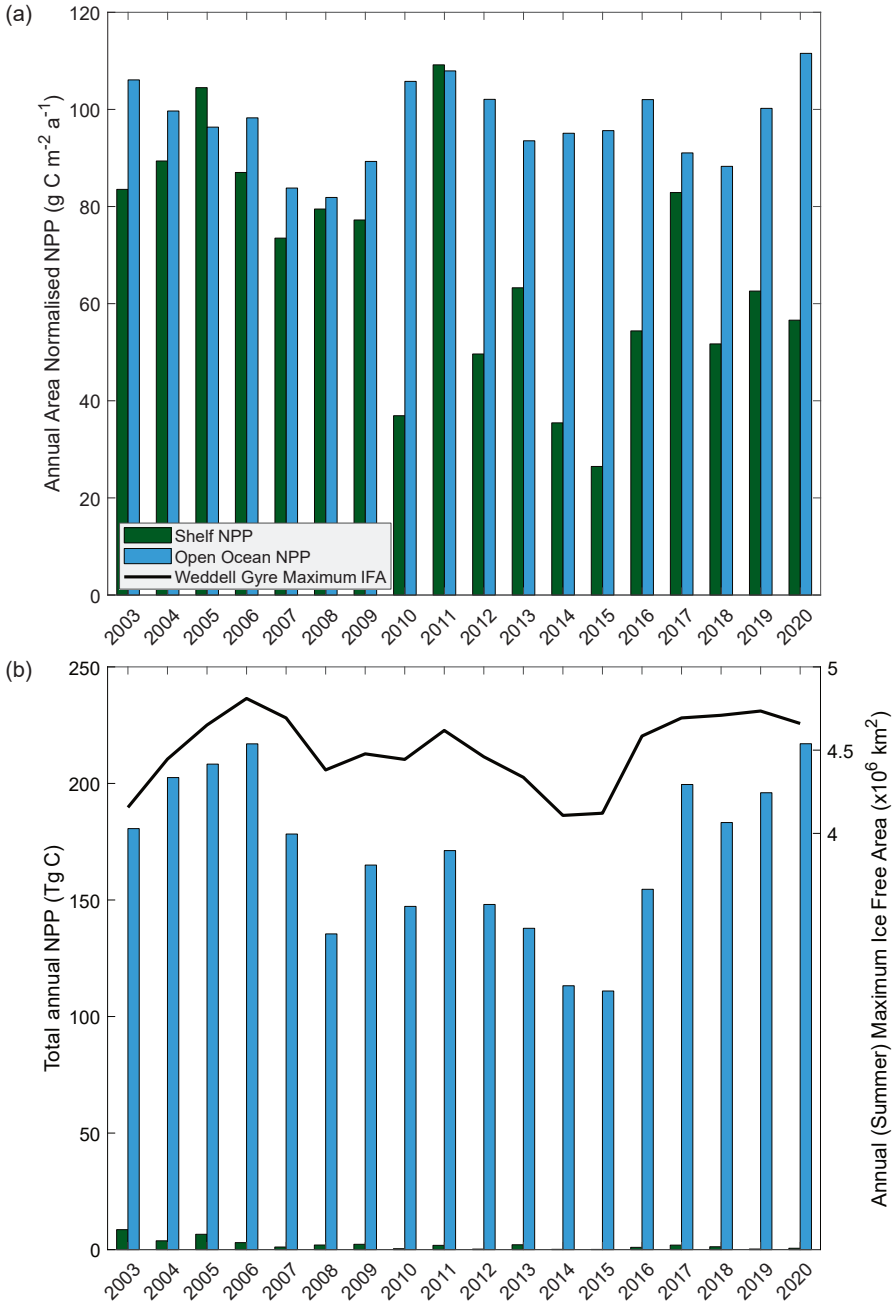

Figure 2. Annual NPP: a) Area-Normalised Annual NPP; b) Total Annual NPP shown on the left axis and Annual (Summer) Maximum Ice Free Area on the right axis. The green bars represent the shelf region value and blue bars for open ocean values.

https://doi.org/10.5194/egusphere-2023-1068
Preprint. Discussion started: 16 June 2023
© Author(s) 2023. CC BY 4.0 License.

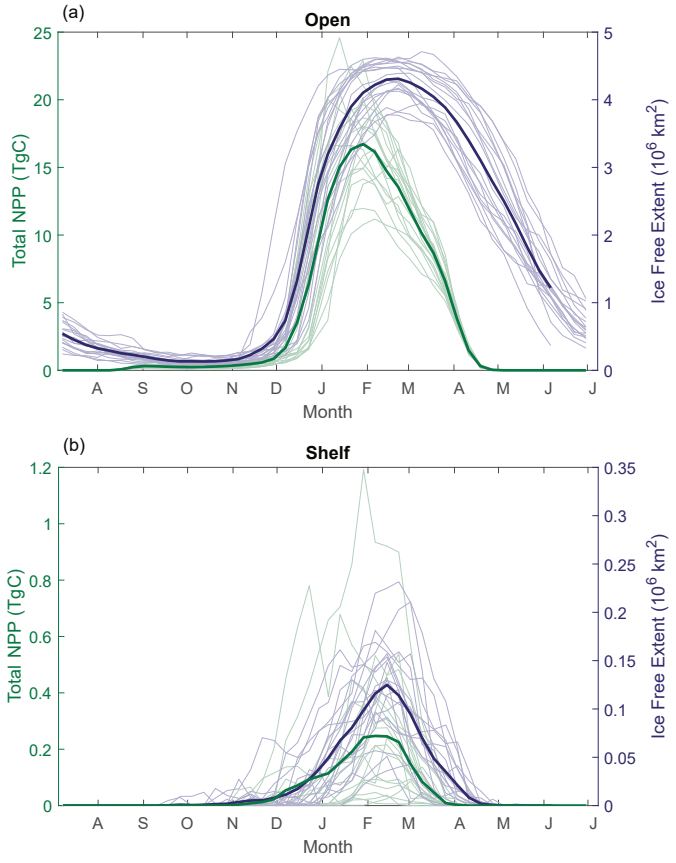

Figure 3. Seasonal cycles of total time-integrated NPP (green) and ice-free Extent (blue) across the (a) open ocean and (b) shelf region. Bold lines represent the 18-year mean, and thin lines show the annual variability.

3.2 Inter-annual variability and trends

185 No secular trends in total annual NPP were observed in the Weddell Gyre or the open-ocean region. Inter-annual variability is large, with production over the austral year in 2006 reaching 220 Tg C, while only 111 Tg C in 2015 (Fig.2.B). Successive NPP minima in 2008 and 2014-2015 may indicate a cyclical pattern with a period of 6-7 years, but a longer timeseries is needed to determine this conclusively. Likewise, no secular trend was observed in any of the sea-ice variables within the Weddell Gyre or open ocean over the study period.

190 In contrast, trends in NPP and sea-ice are seen in the shelf region. Total annual NPP on the shelf has significantly declined during the study period (average decrease of 5% per year, $p<0.01$). As with total NPP, the annual summer maximum IFA has decreased across the shelf region by 1.3% per year on average. However, these trends are sensitive to the occurrence of

https://doi.org/10.5194/egusphere-2023-1068
Preprint. Discussion started: 16 June 2023
© Author(s) 2023. CC BY 4.0 License.

extremes in the early part of the time-period when there were polynyas along the Antarctic Penisula. No trend is seen in the shelf NPP nor IFA when these first 3 years are removed from analysis.

Pearson correlation tests were carried out to determine the correlation between NPP and IFA. Single and multiple linear regressions were then performed to assess the individual and combined effects of time and open water area on total annual NPP. Summer maximum IFA represents the largest area that is available for NPP to occur in a year. Furthermore, because the winter sea-ice edge in the Atlantic sector largely extends beyond the Weddell Gyre boundaries used in this current study region, the maximum IFA (minimum SIA) is also an indicator of the total area of SI retreat in a year. Regression analysis shows a significant relationship between the annual maximum IFA and total NPP, indicating that years with greater IFA result in more total NPP (Fig. 4). In the Weddell Gyre, 62% of the inter-annual variability in total annual NPP can be explained by variability in the summer maximum IFA. Within the sub-regions, this relationship was strongest in the open ocean region, with 55% of the variance in total annual NPP explained by the summer maximum IFA (Fig. 4). In the shelf region, 40% of the variability in total NPP is explained by the yearly maximum IFA. As with the timeseries trends, the first three years had a large influence on the fitted regression model for the shelf region, as indicated by high Cook's Distance values. The effect of the annual maximum IFA on NPP within the shelf region was weakened when the first three years were removed from the regression (R^2=0.34,p=0.01).

In the open ocean, and in the Weddell Gyre as a whole, the area-normalised annual mean NPP for each region is not correlated with any sea-ice variables. However, the shelf region sees positive correlations between area-normalised annual mean NPP and mean IFA (R^2=0.66; p=0.002), sea-ice retreat (R^2=0.58; p=0.011), and mean visible days (R^2=0.76; $p<0.001$). This correlation indicates that NPP in the shelf region is more intense when there is greater IFA. It is plausible that this correlation arises from the spatial dependence of NPP intensity in the shelf region, *i.e.* more IFA consistently indicates that a region with particularly intense production has been exposed.

Across the Weddell Gyre, and throughout the measurement period, a wide range of "satellite-visible days" were recorded. The mean number of satellite-visible days (days where the surface ocean is both ice-free and visible to MODIS-Aqua before the solar angle restricts satellite observations) across the open ocean was 92 days, but due to the size of the region and the rate of sea-ice retreat, there was a large range in the number of satellite visible days seen at any given satellite pixel across the open ocean in any given year (0-260). The mean duration that the shelf region was visible to ocean-colour satellites was 35 days (range of 0-135 days for individual satellite pixels in individual years). Thus, on a pixel-by-pixel basis, we can further assess the relationship between ice cover (visible days) and NPP. The annual area-normalised NPP in any location (pixel) is significantly correlated to the length of time it is visible to the ocean-colour satellite during the year. Fig.5 shows that, in general, locations that are visible to the ocean-colour satellite report greater annual NPP than locations which were visible for fewer days. However, in the open ocean, the rate of increase slows beyond $\sim$120 ice-free days (when the linear and asymptotic lines cross/diverge). In the shelf region, the increase in NPP when visible for longer is greater than in the open ocean (one-tailed t-test (34 df) = -6.195,$p<0.005$), suggesting a more rapid response to earlier ice melt/longer ice-free (satellite visible) periods. However, it is notable that in the density distribution, the majority of the pixels are only observable for very short periods, and importantly, seldom longer than 100 days.

https://doi.org/10.5194/egusphere-2023-1068
Preprint. Discussion started: 16 June 2023
© Author(s) 2023. CC BY 4.0 License.

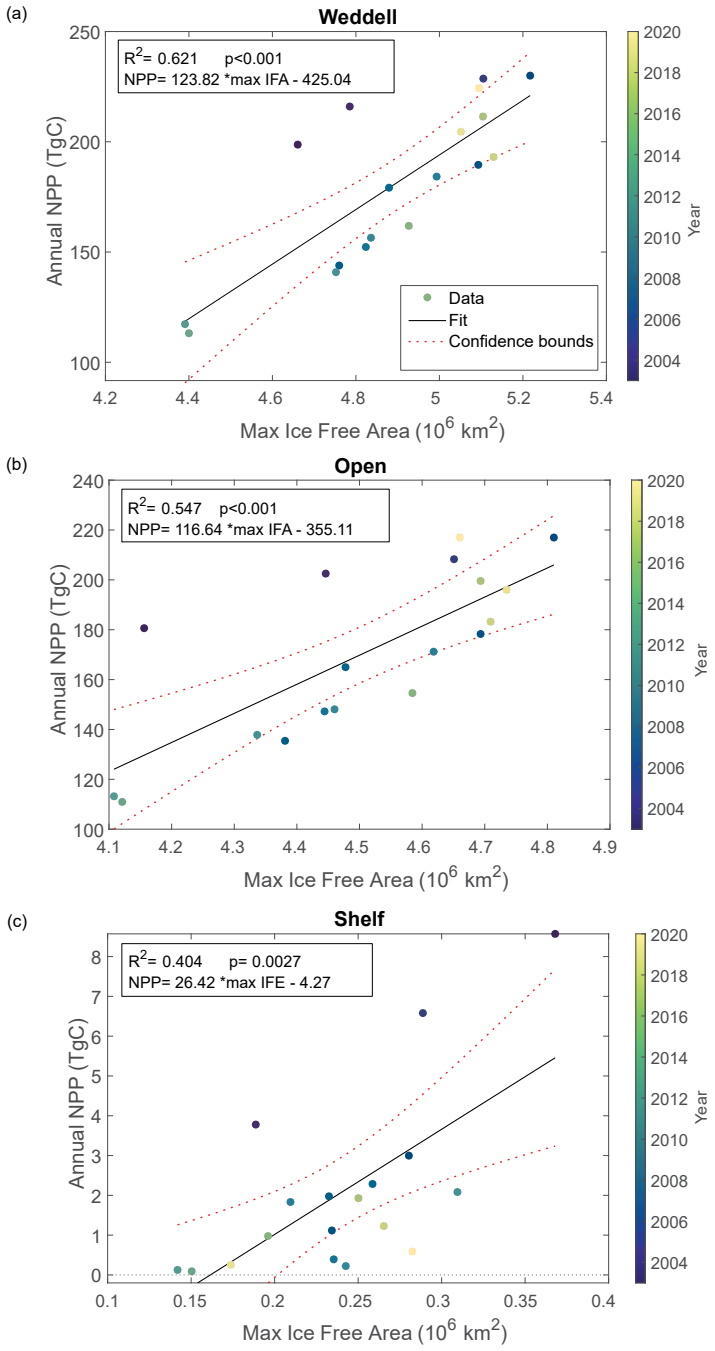

Figure 4. Relationship between annual maximum ice-free area and annual NPP: The variability in the maximum area of ice-free water each year explains the inter-annual variability in total NPP across the Weddell Gyre and each of the subregions.

https://doi.org/10.5194/egusphere-2023-1068
Preprint. Discussion started: 16 June 2023
© Author(s) 2023. CC BY 4.0 License.

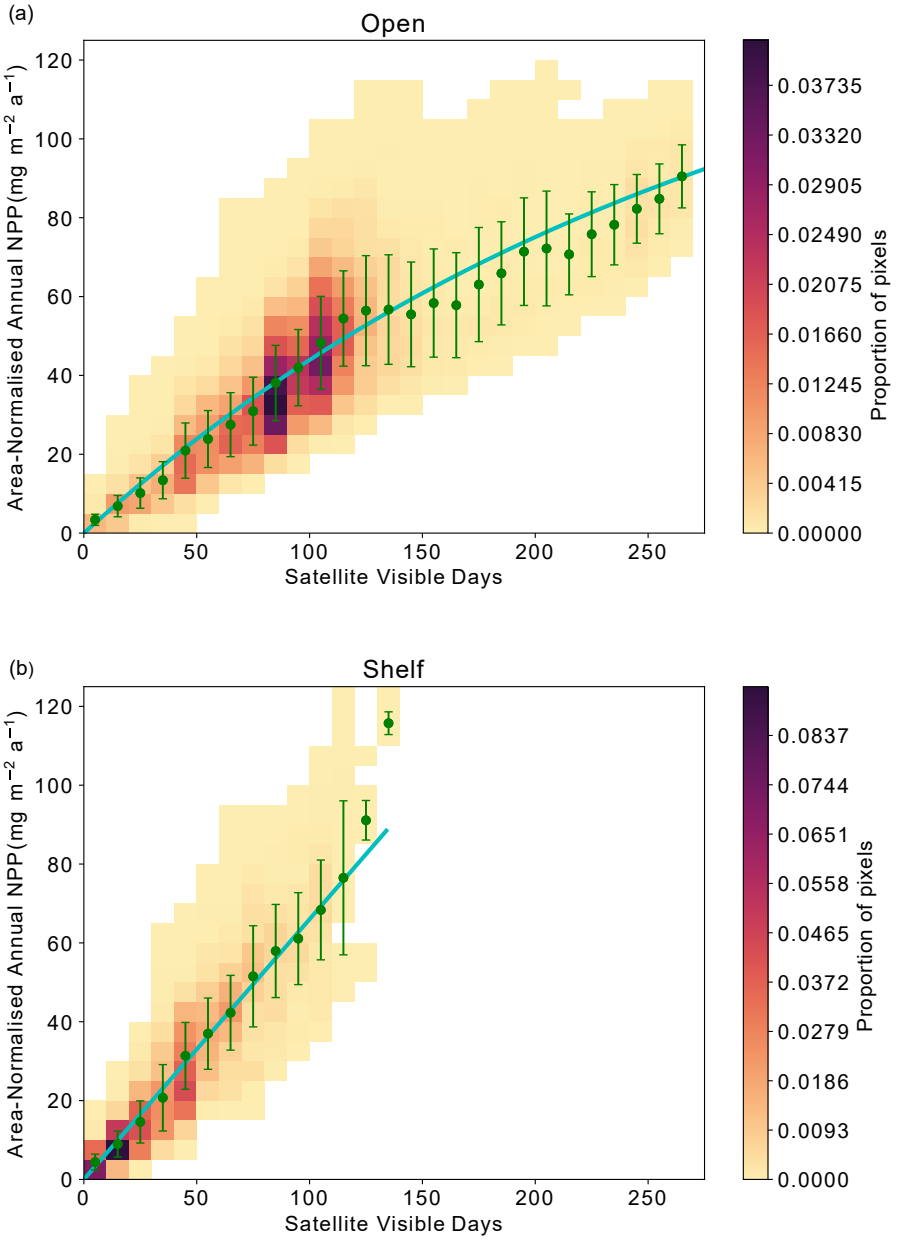

Figure 5. Relationship between area-normalised annual NPP and number of visible days (VD) for all satellite data pixels over the timeseries. Heatmap shows the area-normalised density distribution of data points, while the lines show the (a) non-linear (open ocean) and (b) linear (shelf) relationships for the whole timeseries. VD bin means ± standard deviation are plotted in green.

https://doi.org/10.5194/egusphere-2023-1068
Preprint. Discussion started: 16 June 2023
© Author(s) 2023. CC BY 4.0 License.

3.3 Aligning satellite and subsurface perspectives

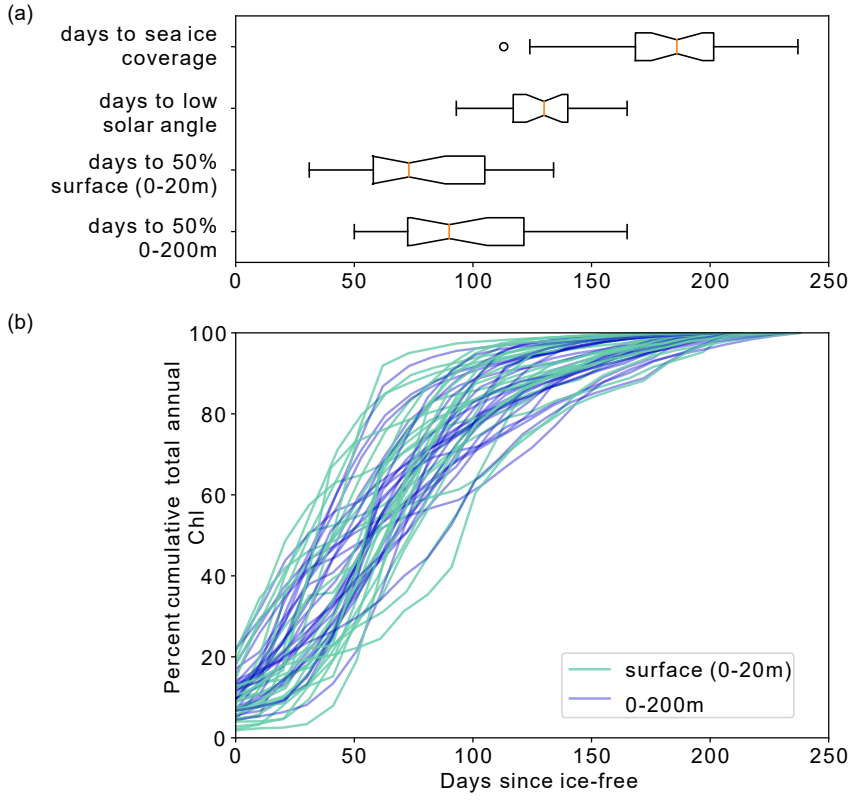

Figure 6. Percent cumulative Chlorophyll-a in the surface (0-20m) and between 0-200m for all completed annual cycles by the floats between 2015-2021. Upper panel indicates the range in the number of days from ice melt to (i) sea-ice return, (ii) low solar angle (loss of satellite observations), (iii) surface bloom end and (iv) depth-integrated bloom end.

Satellite observations indicate that, in the open ocean, the strong positive correlation between visible days and NPP degrades after around 120 visible days, indicating that other processes (e.g. grazing, nutrient availability) begin to limit NPP after this much exposure. To complement and deepen this analysis, we seek to address the same question in the available float observations. Although these data come from drifting platforms, rather than fixed points, we can enquire how the seasonal

https://doi.org/10.5194/egusphere-2023-1068
Preprint. Discussion started: 16 June 2023
© Author(s) 2023. CC BY 4.0 License.

cycle of Chl-a unfolds in each year, and specifically how it evolves relative to light availability. It is worth noting that, due to the depth restrictions of floats, these data all represent open ocean conditions.

Figure 6 shows the progression of the bloom for each year for each float, starting at the first ice-free day (bottom panel). We evaluate the bloom progression for both the surface (0 to 20m; analogous to satellite-observed depths) and upper 200m, and define the bloom end as the date that Chl-a concentrations declined and remained below 50% of their seasonal maximum. Across all years and floats, median surface bloom end occurred 85 days after ice melt (range 41-144 days), while median depth-integrated bloom ended on day 96 following ice melt (range 50-155 days; Fig. 6, upper panel). The later date of bloom end for the depth-integrated values indicates that, on average, primary production in the water column continued at depth until slightly later in the season.

A significant decline of the bloom consistently occured prior to the low solar angle and substantially before the return of ice coverage (Fig. 6; upper panel). Overall, surface bloom ends preceded low solar angle by median 50 days (range: 100 days before to 10 days after) and preceded ice coverage by median 130 days (range: 176 days before to 0 days). Surface and depth-integrated blooms ended before the date of low solar angle and the date of sea-ice return in all but one of the 23 float-years. This supports the supposition inferred from the satellite data that, in regions experiencing an extended period of ice-free days, NPP becomes limited by factors other than light.

4 Discussion

4.1 Biological carbon uptake in the Weddell Gyre dominated by NPP in open ocean region

This study shows that over the last 18 years, open ocean productivity has a dominant role in the carbon cycle of the Weddell Gyre, in agreement with synoptic ship-based studies (MacGilchrist et al., 2019; Brown et al., 2015). MacGilchrist et al. (2019) documented that the region was a net annual CO_2 sink only due to a large amount of carbon sourced from biological activity in the central gyre accumulating in the local Circumpolar Deep Water; horizontal circulation of this water mass out of the Weddell Gyre then facilitates sequestration of carbon over long time scales.

Nevertheless, many studies of Weddell Gyre productivity have focused on the shelf and coastal regions surrounding Antarctica because of the high local rates of NPP and the importance of deep-water formation for carbon export (Arrigo et al., 2008a, 2015; Yager et al., 2016). While we find similarly high rates of coastal NPP, we additionally show that the SIZ beyond coastal areas also exhibits considerable biological carbon uptake. This is in agreement with Arrigo et al. (2008b), who found that rates of productivity in the recently uncovered waters of the marginal ice zone can be as high as polynyas and shelf systems. They also identified the Weddell Sea marginal ice zone as the largest and most productive marginal ice zone of all the geographic sectors investigated (25% greater than the Ross Sea marginal ice zone; Arrigo et al., 2008b), emphasising the importance of this region to the SO biological carbon pump.

Our current study highlights the importance of the Weddell Gyre's open ocean compared to the shelf region, showing that the majority (99%) of the carbon uptake by phytoplankton in the Weddell Gyre occurs there, despite higher daily rates of NPP

https://doi.org/10.5194/egusphere-2023-1068
Preprint. Discussion started: 16 June 2023
© Author(s) 2023. CC BY 4.0 License.

observed on the shelf. This is due to its far greater areal extent (an order of magnitude larger than the shelf region) and much longer ice-free growing season.

4.2 Drivers of NPP variability

Our results show a clear relationship between sea-ice and NPP on an inter-annual timescale (Fig. 5). A large fraction of this likely arises from the role of sea-ice cover in setting light availability in the SIZ. We discuss the nature of this relationship (which accounts for 40-55% of the variance in NPP) in the following section, before exploring other possible sources of interannual variability.

4.2.1 Sea-ice as a control of light availability

Light availability is restricted under sea-ice, so when sea-ice retreats, light limitation caused by sea-ice coverage is alleviated (Twelves et al., 2021; Arrigo and Van Dijken, 2011; Arrigo et al., 2015; Rohr et al., 2017; Smith and Comiso, 2008). Therefore, while the annual NPP cycle at high latitudes is generally driven by regular seasonal changes in solar angle/position through the year (Ardyna et al., 2017; Arrigo et al., 2008b; Park et al., 2017; Smith and Comiso, 2008), within the SIZ, the initiation of growth and the total NPP that results is also mediated by sea-ice cover and its inter-annual variability (Rohr et al., 2017; Twelves et al., 2021). Satellite and float data presented here reflect this: in Fig. 3, where the increase in total NPP from late November mirrors the retreat of sea-ice (increase in the IFA); and in Figures 6, A2, A3, where float profiles show that the majority of growth occurs after floats become ice-free (in spite of Chl-a in the water column starting to increase while floats are still under ice). In an aggregated sense, our basin-scale analysis of the Weddell Gyre confirms that the variability in the sea-ice coverage over the timeseries is a dominant driver of the inter-annual variability in NPP: annual summer minimum SIA (summer maximum IFA) in particular explains 40-55% of the NPP variability within the subregions and 60% of NPP variance in the Weddell Gyre overall (Fig. 4). This finding is consistent with the suggestion that larger areas of ice-free water provide more space for NPP to take place (Arrigo et al., 2008b, 2015).

Some of the unexplained variance in NPP could be related to the spatial pattern of sea-ice retreat. Daily average NPP exhibits substantial spatial variations (not shown), with “hot spots“ around Maud Rise, along the narrow shelf in the east, and in the open ocean near the eastern boundary of the Gyre. These hotspots are thought to be set by comparatively high levels of nutrient supply (e.g. Vernet et al., 2019; Geibert et al., 2010; Arrigo et al., 2015). Consequently, in any given year, spatial variations in where and when sea-ice retreats will determine whether or not these hot spot regions are exposed and for how long, with concomitant impacts on integrated carbon uptake across the Weddell Gyre.

Inter-annual variability in sea-ice cover is set by physical mechanisms, such as atmospheric forcing (e.g. phase of the Southern Annular Mode) and ocean forcing (e.g. sea surface temperature) (Kumar et al., 2021). Recent work has shown that seasonal to inter-annual variability in Antarctic sea-ice cover exhibits substantial predictability (Libera et al., 2022; Bushuk et al., 2021). The strong relationship seen here between sea-ice and NPP therefore indicates that sea-ice predictability may translate into predictability of NPP, with consequences for fisheries and ecosystem management. Indeed, this link between sea-ice and NPP predictability was recently shown in a perfect model context (Buchovecky et al.).

https://doi.org/10.5194/egusphere-2023-1068
Preprint. Discussion started: 16 June 2023
© Author(s) 2023. CC BY 4.0 License.

At a local level, area-normalised NPP appears strongly related to the duration that an area has sufficient available light (Fig. 5; see Sect. 2.4 for a discussion on the distinction between visible days and light availability). Over shelf sea regions, sea-ice persists for longer and reforms earlier than in the open ocean, meaning that the duration of light availability is set by both the retreat and return of sea-ice (Fig. 3). The strongly linear relationship in Fig. 5 suggests that phytoplankton on the shelf are primarily limited by light availability, itself controlled by sea-ice cover. This is consistent with the expectation that the shelf sea regions are nutrient (specifically iron) replete (Arrigo et al., 2015; Boyd et al., 2012; McGillicuddy et al., 2015; Sedwick and Ditullio, 1997), such that they do not become nutrient limited during the short ice-free season. In the open ocean, the earlier melt and later return of sea-ice (Fig. 3) means that the number of visible days can be much longer (Fig. 5). Consequently, we can see a tapering of the relationship to NPP (Fig. 5) indicating that other factors in the open ocean, such as nutrient availability or top-down controls, mediate NPP towards the end of the growing season, and thus impact its interannual variability.

The sub-surface float data further support the finding that factors other than light impact NPP towards the end of the growing season in the open ocean. For the majority of float years, a decline in Chl-a occurs before light limitation returns (Fig. 6) – i.e. before the solar angle is below critical (20°) in March, and well in advance of the return of sea-ice to the float's location. The average timing of this decline (73 days at the surface) is broadly consistent with what is seen in the satellite results. The implication is that the decline in growth after 2-3 months of ice-free conditions leads to a suppression in annually integrated NPP in areas where the ice-free season lasts longer than approximately 3-4 months.

4.2.2 Iron

In the open ocean subregion, once the sea-ice is gone, other factors – such as nutrient supply – determine how much NPP takes place, and for how long (Fig. 5). We hypothesise that the open ocean experiences a progression from light limitation when sea-ice is present, to nutrient limitation once the ice-free season has persisted longer than 80-120 days (Figures 5,6). This picture is consistent with other studies that identify a progression of limiting factors in the SO (Arrigo et al., 2015; Ryan-Keogh et al., 2017; Sedwick et al., 2011; Twelves et al., 2021; von Berg et al., 2020). Thus, nutrient limitation could be setting an upper limit to NPP and effectively dampen the influence of sea-ice on interannual variability, particularly in areas that experience longer ice-free seasons.

The hypothesis that nutrient limitation is the factor controlling NPP in areas of long ice-free seasons is well supported by existing literature. Much of the SO is macro-nutrient replete but micronutrient limited (primarily by iron (de Baar et al., 1995; Hauck et al., 2015) and possibly by manganese (Hawco et al., 2022). Some areas also experience silicate limitation after the spring bloom (Lafond et al., 2020; Quéguiner, 2013), although this is unlikely in the Weddell Gyre, as high concentrations of silicate have been documented through extensive repeat sections through the region (Hoppema et al., 2015). Iron limitation has been found to be more prevalent with distance from the ice shelf, as well as later in the growing season, when the 'winter inventory' has been utilised (Twelves et al., 2021; Boyd et al., 2012; Hoppema et al., 2007). In the Weddell Gyre, the areas that have the longest ice-free/satellite-visible seasons are also generally the areas furthest from the ice shelf and continent, and therefore furthest from an abundant iron supply. We postulate therefore that iron limitation is a major driver of the slowing/decline in NPP that occurs prior to sea-ice return in the open ocean (Figures 3, and 5).

https://doi.org/10.5194/egusphere-2023-1068
Preprint. Discussion started: 16 June 2023
© Author(s) 2023. CC BY 4.0 License.

Our hypothesis of iron limitation at the end of the growing season is supported by the sub-surface Chl-a data observed by floats (Appendix Figure A3). In particular, the continuation of elevated Chl-a close to the base of the mixed layer (Appendix Figure A3) after the cessation of the initial surface bloom indicates that phytoplankton are benefiting from replenishment of nutrients from below the mixed layer through diapycnal mixing (Arrigo et al., 2015; Taylor et al., 2013). Float data suggest that deeper blooms are different in type/composition to those occurring at the surface due to differing persistence (Appendix Figures A2,A3).This further supports the hypothesis that nutrient limitation is playing a major role in phytoplankton growth, although its net impact on NPP cannot be confirmed.

The complexity of the relationship between light and nutrient limitations – and their implications for interannual variability in annual NPP – is exemplified by the occasional occurrence of a secondary (temporally separated) late-summer bloom (Appendix Figure A3. e.g. floats 5904397: 2018, 2019; 5904467: 2018; 5904471: 2018). These secondary blooms typically follow a set pattern (von Berg et al., 2020): when sea-ice melt occurs earlier, iron resources are then also depleted earlier in the growing season. The secondary bloom initiates when micro-nutrients are replenished from entrainment/diapycnal mixing (Arrigo et al., 2015; Taylor et al., 2013), before it is later cut off by a combination of sea-ice return and reduction in PAR due to a shoaling of the light penetration depth (Appendix Figure A3). Two temporally separate blooms are not always visible, with previous studies suggesting that the timing of the first bloom may be a key driver for this (von Berg et al., 2020), otherwise the two blooms will overlap in time sufficiently as to be indistinguishable. Further iron limitation, grazing pressure, or low light levels bring an end to the second bloom. The observation of double blooms, particularly with the latter sometimes occurring at different locations in the water column, indicates that the processes limiting NPP or acting as a brake on its magnitude are not identical in all locations/water depths.

As with sea-ice cover and its impact on light limitation (Sect. 4.2.1), physical mechanisms drive inter-annual variability in nutrient supply, with plausible implications for the variability in annual NPP. Changes in iron supply to the ocean surface and thus the alleviation of iron limitation can occur through variability in mixing (Prend et al., 2022; Biddle and Swart, 2020; Swart et al., 2020), upwelling of iron rich deep waters (Moreau et al., 2023; Twelves et al., 2021; Hoppema et al., 2015; Vernet et al., 2019), as well as supply of icebergs to warmer areas of the gyre (Geibert et al., 2010). Furthermore, in addition to its impact on light availability, sea-ice dynamics play an important role in supplying iron to the SIZ (Boyd et al., 2012), possibly complicating the impact of sea-ice variability on annual NPP.

4.2.3 Other factors limiting NPP

Within the scope of this study, it has not been possible to assess additional controls on phytoplankton growth, beyond sea-ice-induced light availability (Sect. 4.2.1) and nutrients (Sect. 4.2.2). However, it is plausible that other factors could be important for the inter-annual variability of NPP, specifically top-down controls (such as zooplankton grazing or microbial activity). The presence of sea-ice can act to decouple grazers and phytoplankton (Hoppema et al., 2000; Rohr et al., 2017; Smetacek et al., 2004), and as micro-nutrient availability diminishes, grazing may increasingly contribute to the decline of the NPP bloom such that, by late summer, grazer populations may be also exerting top-down control over NPP (Rohr et al., 2017; Smetacek et al., 2004). Vernet et al. (2019) review various studies that have highlighted the abundance of higher trophic levels

https://doi.org/10.5194/egusphere-2023-1068
Preprint. Discussion started: 16 June 2023
© Author(s) 2023. CC BY 4.0 License.

in areas of the Weddell Gyre, and Kauko et al. (2022) recently highlighted krill as exerting top-down (grazing) control on diatom populations in the Kong Håkon VII Hav. However, there is a lack of widespread zooplankton research that has taken place through the Weddell Gyre open ocean, and so it is difficult to determine whether grazers are a significant control of phytoplankton. Variability in ecosystem composition is also likely a significant contribution to the temporal and spatial signal of integrated NPP (Lin et al., 2021; Trimborn et al., 2019; Mascioni et al., 2021; Takao et al., 2020).

4.3 Implications for the future

Sea-ice extent around Antarctica is expected to change in response to anthropogenic global warming (Kumar et al., 2021; Ludescher et al., 2019; Casagrande et al., 2023). With its strong link to NPP, as exhibited in this study, changes in sea-ice dynamics could strongly impact biological carbon uptake in the Weddell Gyre. In turn, this could affect the ecosystem health as well as the contribution that the Weddell Gyre makes to global carbon uptake and climate (Henley et al., 2020).

Our results strongly suggest that, within the SIZ, a larger ice-free area and longer ice-free season (such as might be expected in a warmer world) will lead to higher annual NPP in many regions. However, our results also indicate that beyond a threshold in the length of the ice-free season, NPP will cease to increase at the same rate. Furthermore, by analogy to the permanently open ocean regions in the present-day Southern Ocean (Arrigo et al., 2008b), a region that becomes permanently ice-free in the Weddell Gyre may be expected to become comparatively unproductive. The implication is that while biological carbon uptake might initially increase in an increasingly ice-free Weddell Gyre, it is more than likely that this increase will have an upper limit, with the potential that NPP could decline in the long-term should the region become part of the permanently open ocean zone (Arrigo et al., 2008b).

Our results further indicate that nutrient supply is a key control on this upper limit for NPP in the present day, particularly in the open ocean. An increasingly ice-free Weddell Gyre will see a greater expanse experiencing nutrient limitation late in the growing season. It is unclear whether the same limitations will have a similar effect on NPP in the shelf region should it become increasingly ice-free for longer than is currently seen ($\sim$ 130 days). Consequently, how NPP will change across the Weddell Gyre becomes sensitive to how iron supply will change in the future. Such changes could also be mediated by changes in sea-ice dynamics due to their impact on stratification, mixing and upwelling (Moreau et al., 2023; Hoppema et al., 2015).

5 Conclusions

This study used a complement of satellite and BGC-Argo float data to assess the temporal and spatial variability in NPP and to characterise and quantify the relationship between NPP and sea-ice in the Weddell Gyre. It is clear that sea-ice dynamics are important in driving NPP in this region - both by initiating the seasonal pattern of growth and influencing the variability in annual NPP. Variability in the sea-ice coverage during 2003-2020 accounts for a high degree of the inter-annual variability in NPP, such that more sea-ice melt results in a greater ice-free area where light limitation is alleviated, thus producing a larger productive area for biological activity to take place in. Additionally, the longer an area is ice-free and visible to the satellites, the greater NPP occurs, although results indicate that in the open ocean, NPP is limited before sea-ice coverage resumes. Float

https://doi.org/10.5194/egusphere-2023-1068
Preprint. Discussion started: 16 June 2023
© Author(s) 2023. CC BY 4.0 License.

data suggests that iron limitation may be the main control, but further research is needed to establish the limiting factors in the open ocean. Substantial spatial variability undoubtedly contributes to the variance in NPP, with consistent and sporadic hotspots of biological activity influencing this variability. Other non-sea-ice associated forcing mechanisms likely account for the remaining inter-annual NPP variability. Ultimately, future changes to sea-ice are expected to influence biological activity to a considerable extent. The open ocean of the Weddell Gyre has been shown to be more important than the shelf region in regards to the total NPP occurring each year due to its large spatial area and longer ice-free seasons. Consequently, future research should include studies of off-shore regions of the SIZ to further understanding on the drivers and limitations of SO NPP.

Data availability. Raw data available from: Oregon State www.science.oregonstate.edu/ocean.productivity/ and SOCCOM December 2021 Snapshot https://doi.org/10.6075/J00R9PJW

Code and data availability. Processed data from data sources above and code used to process data and create figures for this paper are available at https://doi.org/10.5281/zenodo.7951184

Appendix A: Supporting Figures

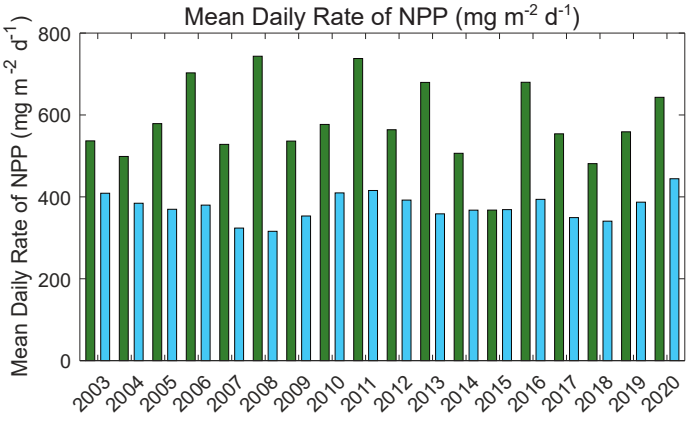

Figure A1. Mean daily NPP. Green bars represent the shelf region value and blue bars for open ocean values.

https://doi.org/10.5194/egusphere-2023-1068
Preprint. Discussion started: 16 June 2023
© Author(s) 2023. CC BY 4.0 License.

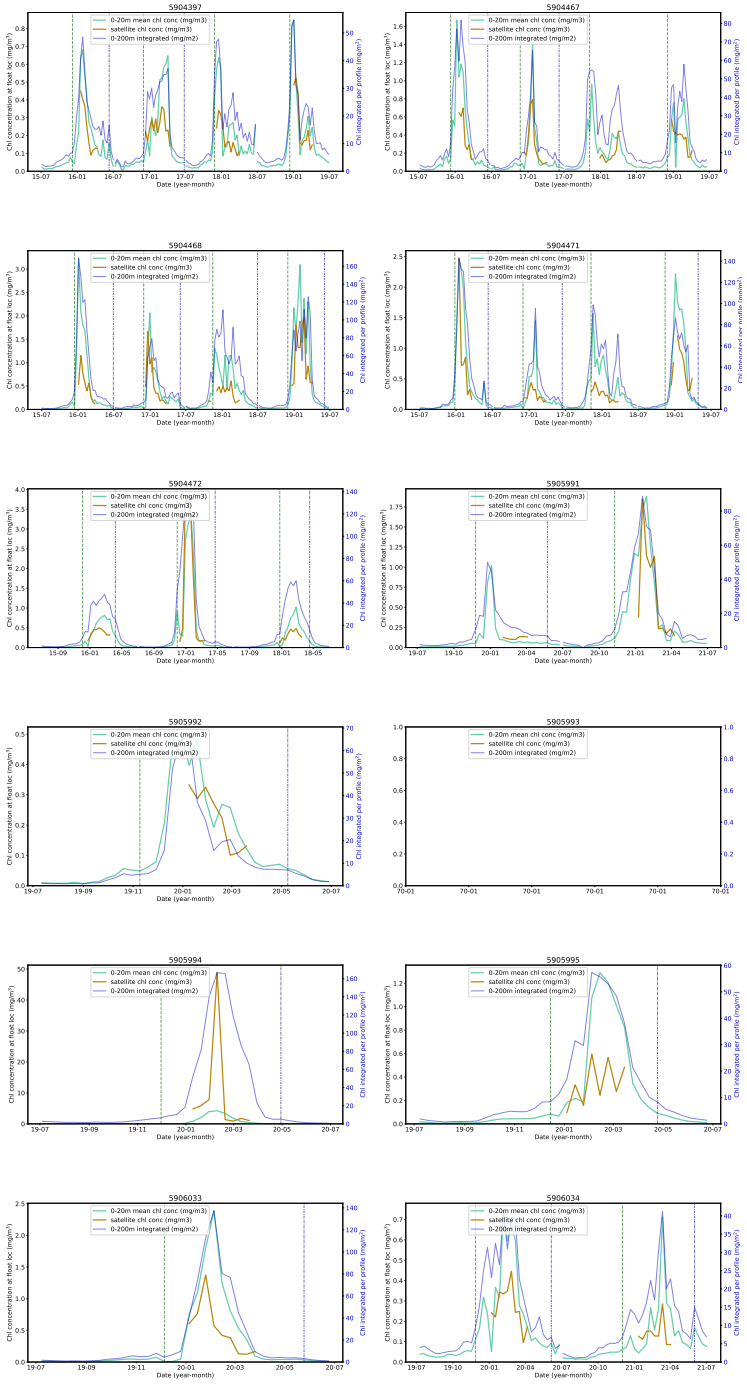

Figure A2. Satellite - float Chlorophyll-a (Chl-a) comparison. Left y-axis mean Chl-a concentration values at (1) the closest pixel to location of float profile (orange line) and (2) between 0-20m (light blue line). Right y-axis shows the integrated Chl-a between 0-200m (dark blue line). Vertical dashed green line indicates start of ice-free season; vertical dash dot blue line indicates start of ice-season.

https://doi.org/10.5194/egusphere-2023-1068
Preprint. Discussion started: 16 June 2023
© Author(s) 2023. CC BY 4.0 License.

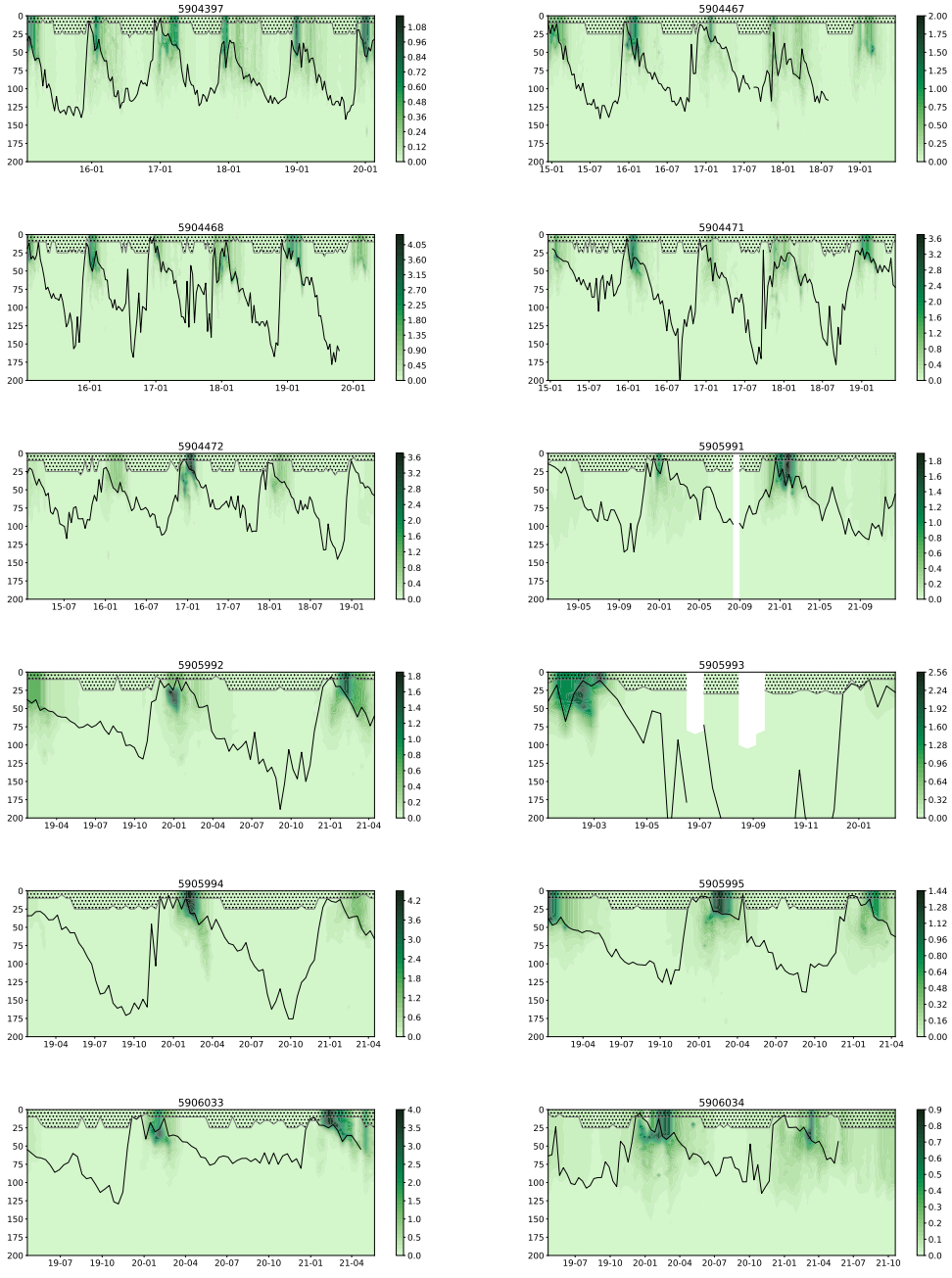

Figure A3. Chlorophyll-a concentration between 0-200m for each float found within the Weddell Gyre study region between 2014-2021. Black line represents the mixed layer depth and shaded areas represent the data extrapolated to the surface from the shallowest float measurement. Note colour scales vary between floats

https://doi.org/10.5194/egusphere-2023-1068
Preprint. Discussion started: 16 June 2023
© Author(s) 2023. CC BY 4.0 License.

Author contributions. Conceptualisation and design of study were carried out by all authors. Data preparation, analysis and writing by CCD. Editing was carried out by all authors.

Competing interests. The authors declare no competing interests.

Acknowledgements. This work was supported by the Natural Environmental Research Council (grant numbers NE/S007210/1 and NE/X008657/1) and by a European Research Council Consolidator grant (GOCART, agreement no. 724416). GAM was supported by the NSF-funded SOC-COM project (PLR-1425989) and UKRI (MR/W013835/1).

https://doi.org/10.5194/egusphere-2023-1068
Preprint. Discussion started: 16 June 2023
© Author(s) 2023. CC BY 4.0 License.

References

Ardyna, M., Claustre, H., Sallée, J. B., D'Ovidio, F., Gentili, B., van Dijken, G., D'Ortenzio, F., and Arrigo, K. R.: Delineating environmental control of phytoplankton biomass and phenology in the Southern Ocean, Geophysical Research Letters, 44, 5016–5024, https://doi.org/10.1002/2016GL072428, 2017.

Arrigo, K. R. and van Dijken, G. L.: Annual cycles of sea ice and phytoplankton in Cape Bathurst polynya, southeastern Beaufort Sea, Canadian Arctic, Geophysical Research Letters, 31, 2–5, https://doi.org/10.1029/2003GL018978, 2004.

Arrigo, K. R. and Van Dijken, G. L.: Secular trends in Arctic Ocean net primary production, Journal of Geophysical Research: Oceans, 116, https://doi.org/10.1029/2011JC007151, 2011.

Arrigo, K. R., van Dijken, G., and Long, M.: Coastal Southern Ocean: A strong anthropogenic CO2 sink, Geophysical Research Letters, 35, 1–6, https://doi.org/10.1029/2008GL035624, 2008a.

Arrigo, K. R., van Dijken, G. L., and Bushinsky, S.: Primary production in the Southern Ocean, 1997-2006, Journal of Geophysical Research: Oceans, 113, 1997–2006, https://doi.org/10.1029/2007JC004551, 2008b.

Arrigo, K. R., Van Dijken, G. L., and Strong, A. L.: Environmental controls of marine productivity hot spots around Antarctica, Journal of Geophysical Research: Oceans, 120, 5545–5565, https://doi.org/10.1002/2015JC010888, 2015.

Arteaga, L. A., Pahlow, M., Bushinsky, S. M., and Sarmiento, J. L.: Nutrient Controls on Export Production in the Southern Ocean, Global Biogeochemical Cycles, 33, 942–956, https://doi.org/10.1029/2019GB006236, 2019.

Bacon, S. and Jullion, L.: RRS James Cook: Antarctic deep water rates of export (ANDREX), Tech. rep., National Oceanography Centre, 2009.

Baldry, K., Strutton, P. G., Hill, N. A., and Boyd, P. W.: Subsurface Chlorophyll-a Maxima in the Southern Ocean, Frontiers in Marine Science, 7, https://doi.org/10.3389/fmars.2020.00671, 2020.

Biddle, L. C. and Swart, S.: The Observed Seasonal Cycle of Submesoscale Processes in the Antarctic Marginal Ice Zone, Journal of Geophysical Research: Oceans, 125, https://doi.org/10.1029/2019JC015587, 2020.

Bisson, K. M. and Cael, B. B.: How are under ice phytoplankton related to sea ice in the Southern Ocean?, Geophysical Research Letters, p. e2021GL095051, https://doi.org/10.1029/2021GL095051, 2021.

Boyd, P. W., Arrigo, K. R., Strzepek, R., and Van Dijken, G. L.: Mapping phytoplankton iron utilization: Insights into Southern Ocean supply mechanisms, J. Geophys. Res, 117, 6009, https://doi.org/10.1029/2011JC007726, 2012.

Boyd, P. W., Claustre, H., Levy, M., Siegel, D. A., and Weber, T.: Multi-faceted particle pumps drive carbon sequestration in the ocean, Nature, 568, 327–335, https://doi.org/10.1038/s41586-019-1098-2, 2019.

Brown, P. J., Jullion, L., Landschützer, P., Bakker, D. C., Naveira Garabato, A. C., Meredith, M. P., Torres-Valdés, S., Watson, A. J., Hoppema, M., Loose, B., Jones, E. M., Telszewski, M., Jones, S. D., and Wanninkhof, R.: Carbon dynamics of the Weddell Gyre, Southern Ocean, Global Biogeochemical Cycles, 29, 288–306, https://doi.org/10.1002/2014GB005006, 2015.

Buchovecky, B., Macgilchrist, G. A., Bushuk, M., Haumann, A., and Fr, T. L.: Potential Predictability of the Spring Bloom in the Southern Ocean Sea Ice Zone, GRL, submitted.

Bushinsky, S. M., Landschützer, P., Rödenbeck, C., Gray, A. R., Baker, D., Mazloff, M. R., Resplandy, L., Johnson, K. S., and Sarmiento, J. L.: Reassessing Southern Ocean Air-Sea CO 2 Flux Estimates With the Addition of Biogeochemical Float Observations, Global Biogeochemical Cycles, 33, 1370–1388, https://doi.org/10.1029/2019GB006176, 2019.

https://doi.org/10.5194/egusphere-2023-1068
Preprint. Discussion started: 16 June 2023
© Author(s) 2023. CC BY 4.0 License.

Bushuk, M., Winton, M., Haumann, F. A., Delworth, T., Lu, F., Zhang, Y., Jia, L., Zhang, L., Cooke, W., Harrison, M., Hurlin, B., Johnson, N. C., Kapnick, S. B., McHugh, C., Murakami, H., Rosati, A., Tseng, K. C., Wittenberg, A. T., Yang, X., and Zeng, F.: Seasonal prediction and predictability of regional antarctic Sea ice, Journal of Climate, 34, 6207–6233, https://doi.org/10.1175/JCLI-D-20-0965.1, 2021.

Campbell, E. C., Wilson, E. A., Kent Moore, G. W., Riser, S. C., Brayton, C. E., Mazloff, M. R., and Talley, L. D.: Antarctic offshore polynyas linked to Southern Hemisphere climate anomalies, Nature, 570, 319–325, https://doi.org/10.1038/s41586-019-1294-0, 2019.

Casagrande, F., Stachelski, L., and de Souza, R. B.: Assessment of Antarctic sea ice area and concentration in Coupled Model Intercomparison Project Phase 5 and Phase 6 models, International Journal of Climatology, https://doi.org/10.1002/joc.7916, 2023.

de Baar, H. J., Bathmannt, U., Smetacek, V., Löscher, B. M., and Veth, C.: Importance of iron for plankton blooms and carbon dioxide drawdown in the Southern Ocean, Nature, 373, 412–415, https://doi.org/10.1038/373412a0, 1995.

Ducklow, H. W., Stukel, M. R., Eveleth, R., Doney, S. C., Jickells, T., Schofield, O., Baker, A. R., Brindle, J., Chance, R., and Cassar, N.: Spring-summer net community production, new production, particle export and related water column biogeochemical processes in the marginal sea ice zone of the Western Antarctic Peninsula 2012-2014, Philosophical Transactions of the Royal Society A: Mathematical, Physical and Engineering Sciences, 376, 20170 177, https://doi.org/10.1098/rsta.2017.0177, 2018.

Geibert, W., Assmy, P., Bakker, D. C., Hanfland, C., Hoppema, M., Pichevin, L. E., Schröder, M., Schwarz, J. N., Stimac, I., Usbeck, R., and Webb, A.: High productivity in an ice melting hot spot at the eastern boundary of the Weddell Gyre, Global Biogeochemical Cycles, 24, https://doi.org/10.1029/2009GB003657, 2010.

Giddy, I., Nicholson, S.-A., Queste, B. Y., Thomalla, S., and Swart., S.: Sea-ice impacts inter-annual variability in bloom phenology and carbon export, ESS Open Archive, https://doi.org/10.1002/essoar.10508727.1, 2021.

Gordon, H. R. and McCluney, W. R.: Estimation of the Depth of Sunlight Penetration in the Sea for Remote Sensing, Applied Optics, Vol. 14, Issue 2, pp. 413-416, 14, 413–416, https://doi.org/10.1364/AO.14.000413, 1975.

Gupta, M., Follows, M. J., and Lauderdale, J. M.: The Effect of Antarctic Sea Ice on Southern Ocean Carbon Outgassing: Capping Versus Light Attenuation, Global Biogeochemical Cycles, 34, https://doi.org/10.1029/2019GB006489, 2020.

Hague, M. and Vichi, M.: Southern Ocean Biogeochemical Argo detect under-ice phytoplankton growth before sea ice retreat, Biogeosciences, 18, 25–38, https://doi.org/10.5194/bg-18-25-2021, 2021.

Hauck, J., Völker, C., Wolf-Gladrow, D. A., Laufkötter, C., Vogt, M., Aumont, O., Bopp, L., Buitenhuis, E. T., Doney, S. C., Dunne, J., Gruber, N., Hashioka, T., John, J., Quéré, C. L., Lima, I. D., Nakano, H., Séférian, R., and Totterdell, I.: On the Southern Ocean CO 2 uptake and the role of the biological carbon pump in the 21st century, Global Biogeochemical Cycles, 29, 1451–1470, https://doi.org/10.1002/2015GB005140, 2015.

Hawco, N. J., Tagliabue, A., and Twining, B. S.: Manganese Limitation of Phytoplankton Physiology and Productivity in the Southern Ocean, Global Biogeochemical Cycles, 36, https://doi.org/10.1029/2022GB007382, 2022.

Henley, S., Cavan, E. L., Fawcett, S. E., Kerr, R., Monteiro, T., Sherrell, R. M., Bowie, A. R., Boyd, P. W., Barnes, D. K. A., Schloss, I. R., Marshall, T., Flynn, R., and Smith, S.: Changing Biogeochemistry of the Southern Ocean and Its Ecosystem Implications, Frontiers in Marine Science, 581, https://doi.org/10.3389/fmars.2020.00581, 2020.

Henson, S. A., Laufkötter, C., Leung, S., Giering, S. L., Palevsky, H. I., and Cavan, E. L.: Uncertain response of ocean biological carbon export in a changing world, Nature Geoscience 2022 15:4, 15, 248–254, https://doi.org/10.1038/s41561-022-00927-0, 2022.

Hindell, M. A., Reisinger, R. R., Ropert-Coudert, Y., Hückstädt, L. A., Trathan, P. N., Bornemann, H., Charrassin, J. B., Chown, S. L., Costa, D. P., Danis, B., Lea, M. A., Thompson, D., Torres, L. G., Van de Putte, A. P., Alderman, R., Andrews-Goff, V., Arthur, B., Ballard, G., Bengtson, J., Bester, M. N., Blix, A. S., Boehme, L., Bost, C. A., Boveng, P., Cleeland, J., Constantine, R., Corney, S., Crawford,

https://doi.org/10.5194/egusphere-2023-1068
Preprint. Discussion started: 16 June 2023
© Author(s) 2023. CC BY 4.0 License.

R. J., Dalla Rosa, L., de Bruyn, P. J., Delord, K., Descamps, S., Double, M., Emmerson, L., Fedak, M., Friedlaender, A., Gales, N., Goebel, M. E., Goetz, K. T., Guinet, C., Goldsworthy, S. D., Harcourt, R., Hinke, J. T., Jerosch, K., Kato, A., Kerry, K. R., Kirkwood, R., Kooyman, G. L., Kovacs, K. M., Lawton, K., Lowther, A. D., Lydersen, C., Lyver, P. O., Makhado, A. B., Márquez, M. E., McDonald, B. I., McMahon, C. R., Muelbert, M., Nachtsheim, D., Nicholls, K. W., Nordøy, E. S., Olmastroni, S., Phillips, R. A., Pistorius, P., Plötz, J., Pütz, K., Ratcliffe, N., Ryan, P. G., Santos, M., Southwell, C., Staniland, I., Takahashi, A., Tarroux, A., Trivelpiece, W., Wakefield, E., Weimerskirch, H., Wienecke, B., Xavier, J. C., Wotherspoon, S., Jonsen, I. D., and Raymond, B.: Tracking of marine predators to protect Southern Ocean ecosystems, Nature, 580, 87–92, https://doi.org/10.1038/s41586-020-2126-y, 2020.

Hoppema, M.: Weddell Sea is a globally significant contributor to deep-sea sequestration of natural carbon dioxide, Deep-Sea Research Part I: Oceanographic Research Papers, 51, 1169–1177, https://doi.org/10.1016/j.dsr.2004.02.011, 2004.

Hoppema, M., Goeyens, L., and Fahrbach, E.: Intense nutrient removal in the remote area off Larsen Ice Shelf (Weddell Sea), Polar Biology, 23, 85–94, 2000.

Hoppema, M., Middag, R., De Baar, H. J., Fahrbach, E., Van Weerlee, E. M., and Thomas, H.: Whole season net community production in the Weddell Sea, Polar Biology, 31, 101–111, https://doi.org/10.1007/s00300-007-0336-5, 2007.

Hoppema, M., Bakker, K., van Heuven, S. M., van Ooijen, J. C., and de Baar, H. J.: Distributions, trends and inter-annual variability of nutrients along a repeat section through the Weddell Sea (1996-2011), Marine Chemistry, 177, 545–553, https://doi.org/10.1016/j.marchem.2015.08.007, 2015.

Johnson, K. S., Plant, J. N., Coletti, L. J., Jannasch, H. W., Sakamoto, C. M., Riser, S. C., Swift, D. D., Williams, N. L., Boss, E., Haëntjens, N., Talley, L. D., and Sarmiento, J. L.: Biogeochemical sensor performance in the SOCCOM profiling float array, Journal of Geophysical Research: Oceans, 122, 6416–6436, https://doi.org/10.1002/2017JC012838, 2017.

Jullion, L., Garabato, A. C., Bacon, S., Meredith, M. P., Brown, P. J., Torres-Valdés, S., Speer, K. G., Holland, P. R., Dong, J., Bakker, D., Hoppema, M., Loose, B., Venables, H. J., Jenkins, W. J., Messias, M. J., and Fahrbach, E.: The contribution of the Weddell Gyre to the lower limb of the Global Overturning Circulation, Journal of Geophysical Research: Oceans, 119, 3357–3377, https://doi.org/10.1002/2013JC009725, 2014.

Kauko, H. M., Assmy, P., Peeken, I., Różańska-Pluta, M., Wiktor, J. M., Bratbak, G., Singh, A., Ryan-Keogh, T. J., and Moreau, S.: First phytoplankton community assessment of the Kong Håkon VII Hav, Southern Ocean, during austral autumn, Biogeosciences, 19, 5449–5482, https://doi.org/10.5194/bg-19-5449-2022, 2022.

Kim, S.-U. and Kim, K.-Y.: Impact of climate change on the primary production and related biogeochemical cycles in the coastal and sea ice zone of the Southern Ocean, Science of the Total Environment, 751, https://doi.org/10.1016/j.scitotenv.2020.141678, 2021.

Kumar, A., Yadav, J., and Mohan, R.: Seasonal sea-ice variability and its trend in the Weddell Sea sector of West Antarctica, Environmental Research Letters, 16, 024 046, https://doi.org/10.1088/1748-9326/abdc88, 2021.

Lafond, A., Leblanc, K., Legras, J., Cornet, V., and Quéguiner, B.: The structure of diatom communities constrains biogeochemical properties in surface waters of the Southern Ocean (Kerguelen Plateau), Journal of Marine Systems, 212, https://doi.org/10.1016/j.jmarsys.2020.103458, 2020.

Libera, S., Hobbs, W., Klocker, A., Meyer, A., and Matear, R.: Ocean-Sea Ice Processes and Their Role in Multi-Month Predictability of Antarctic Sea Ice, Geophysical Research Letters, 49, 1–10, https://doi.org/10.1029/2021GL097047, 2022.

Lin, Y., Moreno, C., Marchetti, A., Ducklow, H., Schofield, O., Delage, E., Meredith, M., Li, Z., Eveillard, D., Chaffron, S., and Cassar, N.: Decline in plankton diversity and carbon flux with reduced sea ice extent along the Western Antarctic Peninsula, Nature Communications 2021 12:1, 12, 1–9, https://doi.org/10.1038/s41467-021-25235-w, 2021.

https://doi.org/10.5194/egusphere-2023-1068
Preprint. Discussion started: 16 June 2023
© Author(s) 2023. CC BY 4.0 License.

Ludescher, J., Yuan, N., and Bunde, A.: Detecting the statistical significance of the trends in the Antarctic sea ice extent: an indication for a turning point, Climate Dynamics, 53, 237–244, https://doi.org/10.1007/s00382-018-4579-3, 2019.

MacGilchrist, G. A., Naveira Garabato, A. C., Brown, P. J., Jullion, L., Bacon, S., Bakker, D. C., Hoppema, M., Meredith, M. P., and Torres-Valdés, S.: Reframing the carbon cycle of the subpolar Southern Ocean, Science Advances, 5, eaav6410, https://doi.org/10.1126/sciadv.aav6410, 2019.

Mascioni, M., Almandoz, G. O., Ekern, L., Pan, B. J., and Vernet, M.: Microplanktonic diatom assemblages dominated the primary production but not the biomass in an Antarctic fjord, Journal of Marine Systems, 224, 103 624, https://doi.org/10.1016/J.JMARSYS.2021.103624, 2021.

McGillicuddy, D. J., Sedwick, P. N., Dinniman, M. S., Arrigo, K. R., Bibby, T. S., Greenan, B. J., Hofmann, E. E., Klinck, J. M., Smith, W. O., Mack, S. L., Marsay, C. M., Sohst, B. M., and Van Dijken, G. L.: Iron supply and demand in an Antarctic shelf ecosystem, Geophysical Research Letters, 42, 8088–8097, https://doi.org/10.1002/2015GL065727, 2015.

Meier, W. N., Fetterer, F., Windnagel, A. K., and Stewart, J. S.: NOAA/NSIDC Climate Data Record of Passive Microwave Sea Ice Concentration, Version 4. 2002-2021, 2021.

Meredith, M., Sommerkorn, M., Cassotta, S., Derksen, C., Ekaykin, A., Hollowed, A., Kofinas, G., Mackintosh, A., Melbourne-Thomas, J., Muelbert, M., Ottersen, G., Pritchard, H., and Schuur, E.: Polar Regions, in: The Ocean and Cryosphere in a Changing Climate, edited by Pörtner, H.-O., Roberts, D., Masson-Delmotte, V., Zhai, P., Tignor, M., Poloczanska, E., Mintenbeck, K., Alegría, A., Nicolai, M., Okem, A., Petzold, J., Rama, B., and Weyer, N., pp. 203–320, Cambridge University Press, https://doi.org/10.1017/9781009157964.005, 2019.

Meredith, M. P.: Cruise report: RRS James Clark Ross JR235/236/239, Tech. rep., British Antarctic Survey, 2010.

Meredith, M. P., Jullion, L., Brown, P. J., Garabato, A. C., and Couldrey, M. P.: Dense waters of the Weddell and Scotia seas: Recent changes in properties and circulation, https://doi.org/10.1098/rsta.2013.0041, 2014.

Moreau, S., Hattermann, T., de Steur, L., Kauko, H. M., Ahonen, H., Ardelan, M., Assmy, P., Chierici, M., Descamps, S., Dinter, T., Falkenhaug, T., Fransson, A., Grønningsæter, E., Hallfredsson, E. H., Huhn, O., Lebrun, A., Lowther, A., Lübcker, N., Monteiro, P., Peeken, I., Roychoudhury, A., Różańska, M., Ryan-Keogh, T., Sanchez, N., Singh, A., Simonsen, J. H., Steiger, N., Thomalla, S. J., van Tonder, A., Wiktor, J. M., and Steen, H.: Wind-driven upwelling of iron sustains dense blooms and food webs in the eastern Weddell Gyre, Nature Communications, 14, 1303, https://doi.org/10.1038/s41467-023-36992-1, 2023.

National Geophysical Data Center/NESDIS/NOAA/U.S. Department of Commerce.: TerrainBase, Global 5 Arc-minute Ocean Depth and Land Elevation from the US National Geophysical Data Center (NGDC)., Research Data Archive at the National Center for Atmospheric Research, Computational and Information Systems Laboratory, Accessed 1, https://doi.org/https://doi.org/10.5065/E08M-4482., 1995.

Park, J., Kuzminov, F. I., Bailleul, B., Yang, E. J., Lee, S. H., Falkowski, P. G., and Gorbunov, M. Y.: Light availability rather than Fe controls the magnitude of massive phytoplankton bloom in the Amundsen Sea polynyas, Antarctica, Limnology and Oceanography, 62, 2260–2276, https://doi.org/10.1002/LNO.10565, 2017.

Peck, L. S., Barnes, D. K., Cook, A. J., Fleming, A. H., and Clarke, A.: Negative feedback in the cold: Ice retreat produces new carbon sinks in Antarctica, Global Change Biology, 16, 2614–2623, https://doi.org/10.1111/j.1365-2486.2009.02071.x, 2010.

Pinkerton, M. H., Boyd, P. W., Deppeler, S., Hayward, A., Höfer, J., and Moreau, S.: Evidence for the Impact of Climate Change on Primary Producers in the Southern Ocean, Frontiers in Ecology and Evolution, 9, 134, https://doi.org/10.3389/fevo.2021.592027, 2021.

Pope, A., Wagner, P., Johnson, R., Shutler, J. D., Baeseman, J., and Newman, L.: Community review of Southern Ocean satellite data needs, Antarctic Science, 29, 97–138, https://doi.org/10.1017/S0954102016000390, 2017.

https://doi.org/10.5194/egusphere-2023-1068
Preprint. Discussion started: 16 June 2023
© Author(s) 2023. CC BY 4.0 License.

Prend, C. J., Keerthi, M. G., Lévy, M., Aumont, O., Gille, S. T., and Talley, L. D.: Sub-Seasonal Forcing Drives Year-To-Year Variations of Southern Ocean Primary Productivity, Global Biogeochemical Cycles, 36, https://doi.org/10.1029/2022GB007329, 2022.

Quéguiner, B.: Iron fertilization and the structure of planktonic communities in high nutrient regions of the Southern Ocean, Deep Sea Research Part II: Topical Studies in Oceanography, 90, 43–54, https://doi.org/10.1016/J.DSR2.2012.07.024, 2013.

Rohr, T., Long, M. C., Kavanaugh, M. T., Lindsay, K., and Doney, S. C.: Variability in the mechanisms controlling Southern Ocean phytoplankton bloom phenology in an ocean model and satellite observations, Global Biogeochemical Cycles, 31, 922–940, https://doi.org/10.1002/2016GB005615, 2017.

Ryan-Keogh, T. J., DeLizo, L. M., Smith, W. O., Sedwick, P. N., McGillicuddy, D. J., Moore, C. M., and Bibby, T. S.: Temporal progression of photosynthetic-strategy in phytoplankton in the Ross Sea, Antarctica, Journal of Marine Systems, 166, 87–96, https://doi.org/10.1016/j.jmarsys.2016.08.014, 2017.

Schultz, C., Doney, S. C., Hauck, J., Kavanaugh, M. T., and Schofield, O.: Modeling Phytoplankton Blooms and Inorganic Carbon Responses to Sea-Ice Variability in the West Antarctic Peninsula, Journal of Geophysical Research: Biogeosciences, 126, e2020JG006 227, https://doi.org/10.1029/2020JG006227, 2021.

Sedwick, P. N. and Ditullio, G. R.: Regulation of algal blooms in Antarctic shelf waters by the release of iron from melting sea ice, Geophysical Research Letters, 24, 2515–2518, https://doi.org/10.1029/97GL02596, 1997.

Sedwick, P. N., Marsay, C. M., Sohst, B. M., Aguilar-Islas, A. M., Lohan, M. C., Long, M. C., Arrigo, K. R., Dunbar, R. B., Saito, M. A., Smith, W. O., and Ditullio, G. R.: Early season depletion of dissolved iron in the Ross Sea polynya: Implications for iron dynamics on the Antarctic continental shelf, Journal of Geophysical Research: Oceans, 116, https://doi.org/10.1029/2010JC006553, 2011.

Séférian, R., Berthet, S., Yool, A., Palmiéri, J., Bopp, L., Tagliabue, A., Kwiatkowski, L., Aumont, O., Christian, J., Dunne, J., Gehlen, M., Ilyina, T., John, J. G., Li, H., Long, M. C., Luo, J. Y., Nakano, H., Romanou, A., Schwinger, J., Stock, C., Santana-Falcón, Y., Takano, Y., Tjiputra, J., Tsujino, H., Watanabe, M., Wu, T., Wu, F., and Yamamoto, A.: Tracking Improvement in Simulated Marine Biogeochemistry Between CMIP5 and CMIP6, Current Climate Change Reports, 6, 95–119, https://doi.org/10.1007/s40641-020-00160-0, 2020.

Sigman, D. M., Hain, M. P., and Haug, G. H.: The polar ocean and glacial cycles in atmospheric CO2 concentration, Nature, 466, 47–55, https://doi.org/10.1038/nature09149, 2010.

Silsbe, G. M., Behrenfeld, M. J., Halsey, K. H., Milligan, A. J., and Westberry, T. K.: The CAFE model: A net production model for global ocean phytoplankton, Global Biogeochemical Cycles, 30, 1756–1777, https://doi.org/10.1002/2016GB005521, 2016.

Smetacek, V., Assmy, P., and Henjes, J.: The role of grazing in structuring Southern Ocean pelagic ecosystems and biogeochemical cycles, Antarctic Science, 16, 541–558, https://doi.org/10.1017/S0954102004002317, 2004.

Smith, W. O. and Comiso, J. C.: Influence of sea ice on primary production in the Southern Ocean: A satellite perspective, Journal of Geophysical Research: Oceans, 113, 1–19, https://doi.org/10.1029/2007JC004251, 2008.

Speer, K. G. and Dittmar, T.: Cruise report, RV Revelle, 33RR20080204, Tech. rep., Florida State University, 2008.

Swart, S., Plessis, M. D., Thompson, A. F., Biddle, L. C., Giddy, I., Linders, T., Mohrmann, M., and Nicholson, S.: Submesoscale Fronts in the Antarctic Marginal Ice Zone and Their Response to Wind Forcing, Geophysical Research Letters, 47, https://doi.org/10.1029/2019GL086649, 2020.

Takao, S., Nakaoka, S. I., Hashihama, F., Shimada, K., Yoshikawa-Inoue, H., Hirawake, T., Kanda, J., Hashida, G., and Suzuki, K.: Effects of phytoplankton community composition and productivity on sea surface pCO2 variations in the Southern Ocean, Deep-Sea Research Part I: Oceanographic Research Papers, 160, https://doi.org/10.1016/j.dsr.2020.103263, 2020.

https://doi.org/10.5194/egusphere-2023-1068
Preprint. Discussion started: 16 June 2023
© Author(s) 2023. CC BY 4.0 License.

Taylor, M. H., Losch, M., and Bracher, A.: On the drivers of phytoplankton blooms in the Antarctic marginal ice zone: A modeling approach, Journal of Geophysical Research: Oceans, 118, 63–75, https://doi.org/10.1029/2012JC008418, 2013.

Trebilco, R., Melbourne-Thomas, J., and Constable, A. J.: The policy relevance of Southern Ocean food web structure: Implications of food web change for fisheries, conservation and carbon sequestration, Marine Policy, 115, 103 832, https://doi.org/10.1016/j.marpol.2020.103832, 2020.

Trimborn, S., Thoms, S., Bischof, K., and Beszteri, S.: Susceptibility of Two Southern Ocean Phytoplankton Key Species to Iron Limitation and High Light, Frontiers in Marine Science, 6, 167, https://doi.org/10.3389/fmars.2019.00167, 2019.

Twelves, A. G., Goldberg, D. N., Henley, S. F., Mazloff, M. R., and Jones, D. C.: Self-Shading and Meltwater Spreading Control the Transition From Light to Iron Limitation in an Antarctic Coastal Polynya, Journal of Geophysical Research: Oceans, 126, e2020JC016 636, https://doi.org/10.1029/2020JC016636, 2021.

Van Heuven, S. M., Hoppema, M., Jones, E. M., and De Baar, H. J.: Rapid invasion of anthropogenic CO2 into the deep circulation of the Weddell Gyre, Philosophical Transactions of the Royal Society A: Mathematical, Physical and Engineering Sciences, 372, https://doi.org/10.1098/rsta.2013.0056, 2014.

Vernet, M., Geibert, W., Hoppema, M., Brown, P. J., Haas, C., Hellmer, H. H., Jokat, W., Jullion, L., Mazloff, M., Bakker, D. C., Brearley, J. A., Croot, P., Hattermann, T., Hauck, J., Hillenbrand, C. D., Hoppe, C. J., Huhn, O., Koch, B. P., Lechtenfeld, O. J., Meredith, M. P., Naveira Garabato, A. C., Nöthig, E. M., Peeken, I., Rutgers van der Loeff, M. M., Schmidtko, S., Schröder, M., Strass, V. H., Torres-Valdés, S., and Verdy, A.: The Weddell Gyre, Southern Ocean: Present Knowledge and Future Challenges, https://doi.org/10.1029/2018RG000604, 2019.

von Berg, L., Prend, C. J., Campbell, E. C., Mazloff, M. R., Talley, L. D., and Gille, S. T.: Weddell Sea Phytoplankton Blooms Modulated by Sea Ice Variability and Polynya Formation, Geophysical Research Letters, 47, https://doi.org/10.1029/2020GL087954, 2020.

Westberry, T. K. and Behrenfeld, M. J.: Oceanic net primary production, in: Biophysical Applications of Satellite Remote Sensing, edited by Hanes, J. M., chap. 8, pp. 205–230, Springer, Berlin, Germany, 2013.

Windnagel, A. K., Meier, W. N., Stewart, J. S., Fetterer, F., and Stafford, T.: NOAA/NSIDC Climate Data Record of Passive Microwave Sea Ice Concentration, Version 4, NSIDC Special Report 20, Boulder CO, https://nsidc.org/data/g02202/versions/4#anchor-1, 2021.

Yager, P., Sherrell, R., Stammerjohn, S., Ducklow, H., Schofield, O., Ingall, E., Wilson, S., Lowry, K., Williams, C., Riemann, L., Bertilsson, S., Alderkamp, A.-C., Dinasquet, J., Logares, R., Richert, I., Sipler, R., Melara, A., Mu, L., Newstead, R., Post, A., Swalethorp, R., and van Dijken, G.: A carbon budget for the Amundsen Sea Polynya, Antarctica: Estimating net community production and export in a highly productive polar ecosystem, Elementa: Science of the Anthropocene, 4, https://doi.org/10.12952/JOURNAL.ELEMENTA.000140, 2016.